



---

THE SCIENCE OF MEASUREMENT

## Technical Report

---

# *SKA-SA Reverberation Chamber Characterisation*

---

Work done for: Square Kilometre Array South Africa



A. J. Otto and P. S. van der Merwe


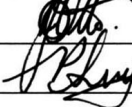
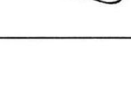
**Document Number:** SKA/13/10/15

**Revision Number:** 0

**Document Date:** 15 October 2013

This document contains proprietary information and may not be disclosed without the written consent of MESA Solutions (Pty) Ltd. or the client whom it is intended for.

## Document Approval

	Name	Affiliation	Designation	Signature
<b>Submitted by</b>	H. C. Reader	MESA Solutions	Director	
	A. J. Otto	MESA Solutions	Associate	
	P. S. van der Merwe	MESA Solutions	Associate	

<b>Accepted by</b>	Mr. S. Norval	SKA South Africa	RFI Manager	

## Document History

Revision	Date of Issue	Comments
0	15 October 2013	Technical Report SKA/13/10/15/REV0

## Company Details

<b>Name</b>	MESA Solutions (Pty) Ltd.
<b>Physical/Postal Address</b>	5 Thierry Street Mostertsdrift Stellenbosch 7600
<b>Tel.</b>	(021) 887 8987
<b>Website</b>	<a href="http://www.mesasolutions.co.za/">http://www.mesasolutions.co.za/</a>

## Executive Summary

MESA Solutions was asked by SKA-SA to evaluate the newly installed *Comtest Engineering* reverberation chamber (RC) at their Pinelands offices. This report considers the practical method for RC characterisation as given in the IEC 61400-4-21 [2]. The main findings are:

- The calibrated chamber yielded a normalised mean E-field variation within  $\pm 1.8$  dB from 200 MHz to 8 GHz.
- The E-field variation is well below the IEC sigma limit for chamber validation.
- The lowest usable frequency of the chamber was calculated, and confirmed, to be approximately 181 MHz.
- The OATS E-field estimation of an emission reference source (ERS) was used to validate the chamber calibration.
- Good correlation between the OATS E-field measured and predicted data of a well-known reference radiator (ERS) was achieved above 400 MHz.
- Further investigation into the sub 400 MHz over-prediction of the ERS-OATS equivalent in the Pinelands SKA-SA RC is currently underway.
- For further validation of the chamber, the  $Z_T$  for a coaxial airline was also measured.
- Good correlation between results for the coaxial airline measured in the RCs of Pinelands and Stellenbosch, compared to the *Vance* theoretical model, was achieved.

## Contents

<b>Executive Summary</b>	<b>2</b>
<b>Nomenclature</b>	<b>4</b>
<b>List of Figures</b>	<b>5</b>
<b>Acknowledgements</b>	<b>6</b>
<b>1 Introduction</b>	<b>7</b>
<b>2 Reverberation Chamber Characteristics</b>	<b>7</b>
2.1 Physical Chamber Dimensions . . . . .	7
2.2 Field Uniformity and Working Volume . . . . .	7
2.3 Frequency Ranges . . . . .	8
2.4 Number of Samples . . . . .	8
2.5 Stirrer Speed Evaluation and E-Field . . . . .	8
2.6 Chamber Attenuation . . . . .	10
2.7 Chamber Loading Factor . . . . .	10
2.8 Field Uniformity Validation . . . . .	10
<b>3 IEC 61000-4-21 Standard Calibration</b>	<b>10</b>
3.1 Calibration Procedure . . . . .	11
3.2 Results . . . . .	13
<b>4 OATS E-Field Equivalent</b>	<b>13</b>
4.1 Initial Tests: ERS and Coaxial Air-Line . . . . .	16
<b>5 RC Metrology</b>	<b>16</b>
5.1 Vector Network Analyzer . . . . .	16
5.2 Pre-Measurement Procedure . . . . .	20
5.3 Measurement Correction . . . . .	20
<b>6 Conclusions</b>	<b>21</b>

## Nomenclature

ACF	Antenna Calibration Factor
CCF	Chamber Calibration Factor
CLF	Chamber Loading Factor
DUT	Device Under Test
E-field	Electric Field
ERS	Emissions Reference Source
FD	Frequency Domain
GHz	Gigahertz
HF	High Frequency
IL	Insertion Loss
LPDA	Log Periodic Dipole Array
LUF	Lowest Usable Frequency
MHz	Megahertz
NPL	National Physica Laboratory
OATS	Open Area Test Site
RC	Reverberation Chamber
SA	Spectrum Analyzer
SKA	Square Kilometre Array
SKA-SA	Square Kilometre Array South Africa
SOLT	Short-Open-Load-Through
TD	Time Domain
TRL	Through-Reflect-Line
VNA	Vector Network Analyzer

## List of Figures

1	Physical dimensions of reverberation chamber: height ( $h$ ), width ( $w$ ) and length ( $l$ ). . . . .	8
2	Measurement setup for stirrer speed evaluation as in [2]. . . . .	9
3	Typical antenna positions at corners of working volume during calibration. . . . .	11
4	Antenna positions at corners of working volume during calibration of the Pinelands SKA-SA RC. . .	12
5	The average E-field measured at the eight positions in the working volume. . . . .	14
6	Normalised E-field to evaluate the field uniformity during chamber calibration. . . . .	14
7	The attenuations of the SKA-SA reverberation chamber: <i>RED</i> is the insertion loss (IL) and <i>BLUE</i> is the chamber calibration factor (CCF). . . . .	15
8	Measured chamber validation compared to the IEC validation requirement limits. . . . .	15
9	Estimation of OATS E-field equivalent for <i>Laplace Instruments LTD</i> emissions reference source. (a) Horizontally polarised radiator. (b) Vertically polarised radiator. (c) Equivalent OATS measurement using the KLPDA in the RC at Stellenbosch University [1]. . . . .	17
10	Geometry of the coaxial airline [1]. . . . .	17
11	OATS E-field estimate from average ( <i>BLUE</i> ) and maximum ( <i>RED</i> ) readings compared to the ERS calibration data ( <i>GREEN</i> ). . . . .	18
12	$Z_t$ of coaxial airline measured in Pinelands and Stellenbosch RCs compared to the theoretical <i>Vance</i> model. . . . .	18
13	Two-port error correction of the 12-term error model [5]. . . . .	19
14	Full 2-port calibration standards [5]. . . . .	20

## Acknowledgements

MESA Solutions would like to acknowledge:

- Mr. Joely A. Andriambeloson for assisting in the measurement campaign.

## 1 Introduction

MESA Solutions was asked by the Square Kilometre Array South Africa (SKA-SA) to evaluate the newly installed *Comtest Engineering* reverberation chamber (RC) at their Pinelands offices (installed by *ITC Services*). For an analytical comprehension of the subject, the modal analysis of RCs was studied in detail in [1]. This report considers the practical method for RC characterisation as given in [2].

## 2 Reverberation Chamber Characteristics

The process of characterising a reverberation chamber requires a two port device such as a vector network analyser (VNA). A VNA makes it possible to excite energy inside the chamber at a particular frequency using one port, and then measure the variation of that energy at the same frequency using a second port. Because the excitation and measurement frequencies are correlated, this process is repeated for a range of frequencies. However, before using the VNA, it has to be calibrated as explained in section 5.1.

### 2.1 Physical Chamber Dimensions

The static chamber is characterised by its cut-off frequency, resonant frequency and number of modes it can produce. The higher the modes that can be produced in the chamber, the higher the probability that the device under test (DUT) will be exposed to the mean electric field (E-field). The total number of modes inside a chamber, governed by the frequency and physical size, is given by:

$$N(f) = \frac{8\pi}{3} w l h \left( \frac{f}{c} \right)^3 - (w + l + h) \frac{f}{c} + \frac{1}{2} \quad (1)$$

The resonant frequency for both transverse magnetic (TM) and transverse electric (TE) modes is given by:

$$F_{mnp} = \frac{1}{2\sqrt{\mu\epsilon}} \sqrt{\left( \frac{m}{w} \right)^2 + \left( \frac{n}{h} \right)^2 + \left( \frac{p}{l} \right)^2} \quad (2)$$

The cut-off frequencies for the TM<sub>101</sub> and TE<sub>110</sub> modes are given by Eqs. 3 and 4 respectively.

$$F_{110} = \frac{1}{2\sqrt{\mu\epsilon}} \sqrt{\left( \frac{1}{w} \right)^2 + \left( \frac{1}{h} \right)^2} \quad \text{TM Mode} \quad (3)$$

$$F_{101} = \frac{1}{2\sqrt{\mu\epsilon}} \sqrt{\left( \frac{1}{w} \right)^2 + \left( \frac{1}{l} \right)^2} \quad \text{TE Mode} \quad (4)$$

The physical dimensions of the RC installed at the Pinelands offices, as given in Fig. 1, are  $w = 2.8$  m,  $l = 5.35$  m and  $h = 2.1$  m. From the dimensions the lowest usable frequency (LUF) can be calculated by determining the fundamental cut-off frequency for the transverse electric (TE) mode of the chamber according to Eq. 4. It is specified in [2] that the LUF is slightly higher than three times the first chamber resonance, therefore:  $181.27\text{MHz} \leq \text{LUF} \leq 241.69\text{MHz}$ .

### 2.2 Field Uniformity and Working Volume

The RC generates a uniform field level inside a volume of the room known as the *working volume*. This region is typically defined as  $\lambda/4$  from the walls and any metallic structures such as the stirrers at the LUF.



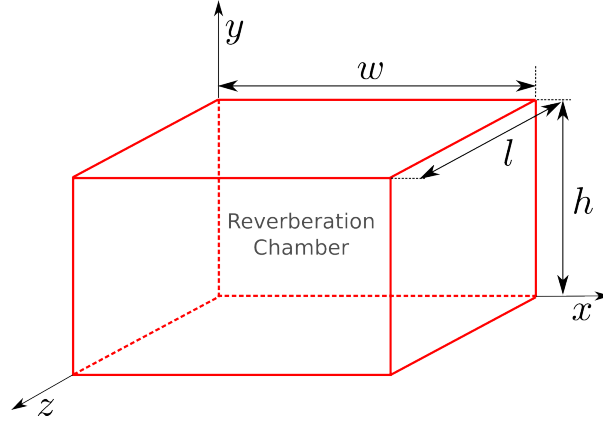


Figure 1: Physical dimensions of reverberation chamber: height ( $h$ ), width ( $w$ ) and length ( $l$ ).

## 2.3 Frequency Ranges

The LUF of the chamber was already determine in section 2.1 based on its physical dimensions. The highest frequency of operation is only limited by the sensitivity of the measuring equipment as chamber attenuation increases with frequency.

## 2.4 Number of Samples

Determining adequate number of samples  $N_S$  should be considered next.  $N_S$  directly influences the number of independent field samples  $N_{Ind}$  obtained during one revolution of the stirrer. The higher  $N_{Ind}$ , the more efficient the stirrer. We can estimate  $N_{Ind}$  by evaluating the autocorrelation coefficient  $\rho$ .

1. The autocorrelation coefficient  $\rho$  given by [1] as:

$$\rho_i = \frac{Cov(X, Y_i)}{\sqrt{Var(X) \cdot Var(Y_i)}} \quad (5)$$

where  $Cov$  and  $Var$  denote the covariance and variance of the random E-field variables  $X$  and  $Y_i$  for  $N_S$  number of samples. The data is considered uncorrelated when  $|\rho| \leq 0.37$

2. Plot  $\rho$  and determine  $\Delta$  where correlation is lost.
3. Calculate  $N_{Ind} = \frac{N_S}{\Delta}$
4. Choose practical  $N_S$  which maximises  $N_{Ind}$

## 2.5 Stirrer Speed Evaluation and E-Field

Synchronisation between the VNA sweeping through the frequency band of interest, and the speed at which the stirrer is rotated, has to be established. The following process can be followed:

1. Position the first antenna (transmitter) at a fixed position on the edge of the working volume. Then move the second antenna (receiver) to two positions A and B inside the working volume as shown in Fig 2.

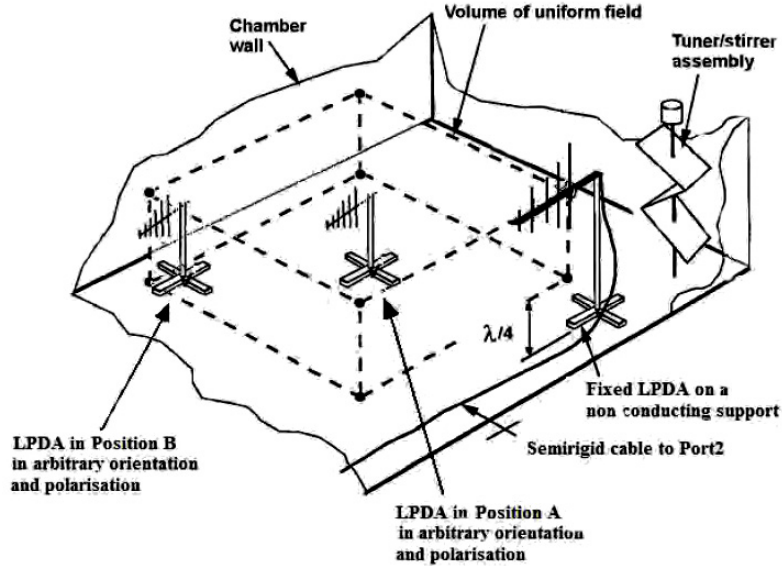


Figure 2: Measurement setup for stirrer speed evaluation as in [2].

2. Determine the time required by VNA to measure the number of samples at each frequency.
3. Determine the time associated with various speeds of stirrer rotation.
4. Compare the different  $S_{21}$  measurements by the VNA for the two locations and different rotational speeds.
5. Calculate the variation in the mean and maximum E-fields in order to determine if the variance is associated with the stirrers or the VNA using Eq. 6.

$$E_{mean} = \sqrt{\frac{\langle P_{Rx} \rangle 8\pi\eta}{\lambda^2}} \cdot \frac{15}{16} \cdot \sqrt{\frac{\pi}{3}} \cdot \frac{\Gamma(3N)\sqrt{3N}}{\Gamma(3N + \frac{1}{2})} \quad (6)$$

where  $\Gamma(X)$  is the factorial function evaluated at  $X$  and  $\eta$  is the the wave impedance in free space.

6. The maximum E-field is given by:

$$E_{max} = \left\langle \frac{8\pi}{\lambda} \cdot \sqrt{5 \frac{P_{maxRx}}{\eta_{Rx}}} \right\rangle_{N \text{ Probe-positions}} \quad (7)$$

where  $P_{maxRx}$  is the maximum received power for one revolution of the stirrer and  $\eta_{Rx}$  is the efficiency of the receive antenna (typicall 0.75 for log periodic dipole array (LPDA) and 0.9 for horn antennas).

## 2.6 Chamber Attenuation

As the signal injected into the chamber reflects off the walls and stirrers, some part of the injected energy is absorbed by the chamber. From the calibration measurements, the attenuation of the input signal due to the chamber can be calculated using the following expression:

$$\text{Att}_{\text{Ch}} = \left\langle \frac{P_{\text{Rx}}}{P_{\text{Tx}}} \right\rangle_{N \text{ probe-positions}} \quad (8)$$

where  $P_{\text{Rx}}$  is the received power at the probe position, and  $P_{\text{Tx}}$  is the power radiated by the transmitting antenna. If  $P_{\text{Rx}}$  is the maximum received power in one revolution, the attenuation is called the antenna calibration factor (ACF). When considering the average received power in one revolution,  $P_{\text{Rx}}$  is known as the chamber insertion loss (IL).

## 2.7 Chamber Loading Factor

When a DUT is placed inside the working volume of the chamber, it affects the chamber characteristics. The DUT changes the field distribution and antenna factor of the empty RC calibration, and is said to *load* the chamber. The effect of the DUT on the chamber can be determined using the loading factor given in Eq. 9. Re-calibrating the chamber with the DUT present in the working volume will give a new attenuation referred to as the chamber calibration factor (CCF).

$$\text{CLF} = \frac{\text{CCF}}{\text{ACF}} \quad (9)$$

## 2.8 Field Uniformity Validation

The chamber will meet the field uniformity requirement of IEC 61000-4-21 standard [2] if the standard deviation of the maximum E-field is within 4 dB below 100 MHz, decreasing linearly to 3 dB at 400 MHz and remains at 3 dB above 400 MHz. This IEC requirement limit is the red plot of the calibration validation given in Fig. 8.

From the calibration data, the maximum E-field at the eight corners of the working volume is calculated using Eq. 7. Thereafter the standard deviation of the E-field at these positions are compared to the IEC requirements for uniformity. From this comparison, we evaluate the frequency range of uniformity, as well as the LUF for the chamber. The standard deviation in [dB] for the E-field is given by Eq. 10.

$$\sigma_{\text{dB}} = 20 \cdot \log_{10} \left( \frac{\sigma + E_{\text{max}}}{E_{\text{max}}} \right) \quad (10)$$

where  $\sigma$  is the *linear* standard deviation and  $E_{\text{max}}$  is the estimated E-field using Eq. 7.

## 3 IEC 61000-4-21 Standard Calibration

The calibration of the RC consists of a number of measurements to determine the signal attenuation and E-field uniformity in the working volume of the chamber. Before the facility is used, the chamber should be calibrated completely empty. The calibration should thereafter be repeated when major modifications, such as stirrer replacement or adjustments, use of absorbers, metallic coating of the wall, or measuring large structures that can load the chamber differently, are made.

Calibration can be done operating the chamber in two modes:

1. Mode-stirred operation:
  - The stirrer is set to rotate freely
  - A set of  $N_S$  samples per frequency are taken during one rotation
2. Mode-tuned operation
  - The stirrer is set to a specific location
  - Frequency range is swept
  - Stirrer is moved to next angle position
  - Process repeated until completion of a full rotation of  $N_S$  samples

At the end of the measurement,  $N_S$  samples are obtained for each frequency. The data is averaged for over these samples to obtain the mean E-field produced in the working volume. The higher the number of samples per revolution, the more accurate the field average.

### 3.1 Calibration Procedure

Eight receiver positions are required to calibrate the chamber. As shown in Fig. 3, these positions are located at the corners of the working volume described in section 2.2.

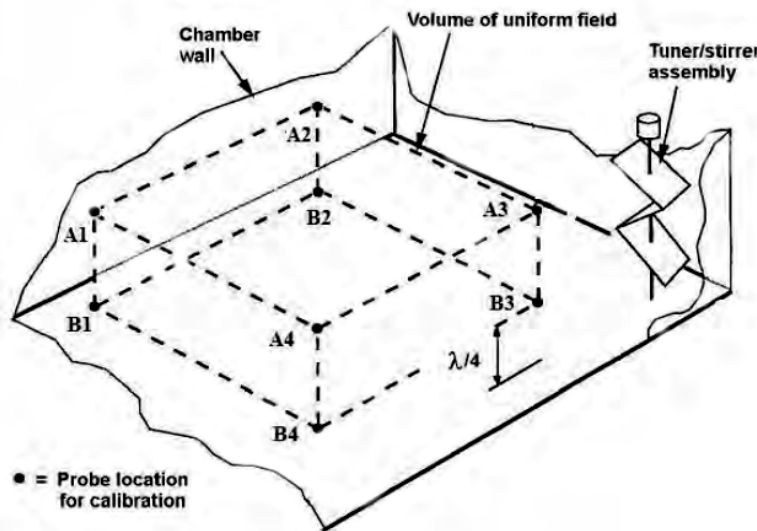


Figure 3: Typical antenna positions at corners of working volume during calibration.

During the calibration, a signal of known power is injected into the chamber at a fixed location within the working volume. Note that the source should not be pointed directly towards the receiver to prevent direct coupling between them. The actual measurement positions using the GLPDA as transmit antenna and KLPDA as receive antenna are shown in Fig. 4.

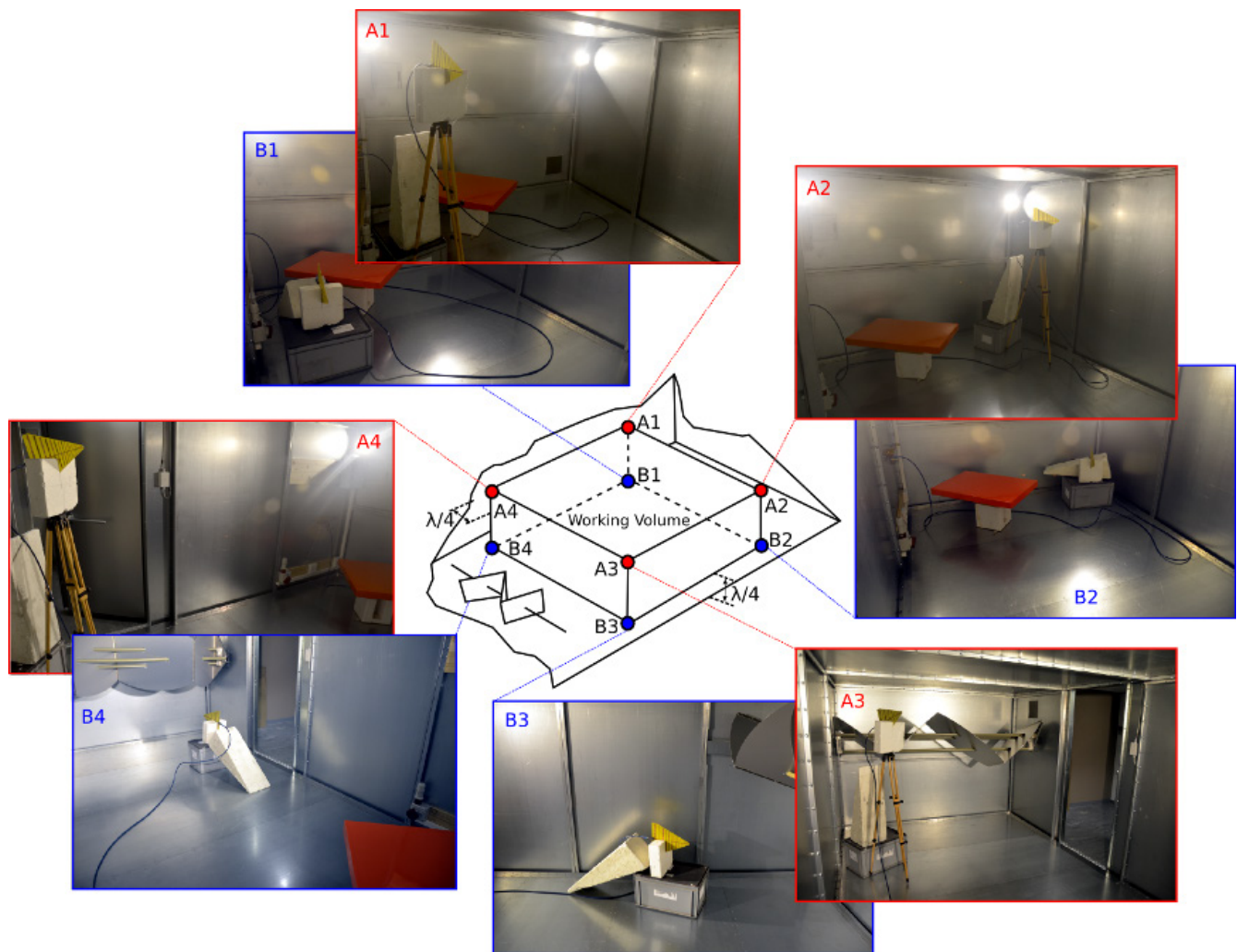


Figure 4: Antenna positions at corners of working volume during calibration of the Pinelands SKA-SA RC.

### 3.2 Results

The average E-field levels measured at the eight positions of the working volume are given in Fig. 5, while the normalised E-fields to evaluate the field uniformity are given in Fig. 6. The insertion loss and chamber characterisation factor are given in Fig. 7, while chamber validation compared to the IEC uniformity requirements are given in Fig. 8.

## 4 OATS E-Field Equivalent

The previous sections explained how to calibrate a reverberation chamber. This process will only be repeated to periodically verify the accuracy of the results, or if a comparatively large object is measured that might significantly load the chamber. Reverberation chambers are used on a more regular basis to determine the total emitted power from a DUT. This power is typically measured using a known-gain antenna and spectrum analyser. Emission measurements can then again be made in either a mode stirred or mode tuned configuration.

The total radiated power for vertical and horizontal polarisations can be compared to the calibrated data for the standard radiator/emissions reference source (ERS) which would typically be measured on an open area test site (OATS). This comparison requires the following:

1. Calculation of the power radiated for the DUT using Eqs. 11 or 12 depending if the average or maximum power per revolution is used.

$$P_{Radiated} = \frac{P_{avg} \eta_{Tx}}{CCF} \quad (11)$$

$$P_{Radiated} = \frac{P_{max} \eta_{Tx}}{CLF \cdot IL} \quad (12)$$

In these equations  $\eta_{Tx}$  is the efficiency of the transmitting antenna.

2. Calculation of the associated radiated E-field (Eq. 13) in which  $D$  is the maximum directivity of the DUT and  $R$  the distance between the device under test and the receiving antenna.

$$E_{radiated} = \sqrt{\frac{D \cdot P_{radiated} \cdot 377}{4\pi R^2}} \quad (13)$$

This is based on the Friis free space equation. The half-space E-field radiation, where the DUT and receiving antenna is placed at a height above a ground-plane, is discussed in [1]. In this scenario the antenna receives two signals: the incident and reflected waves.

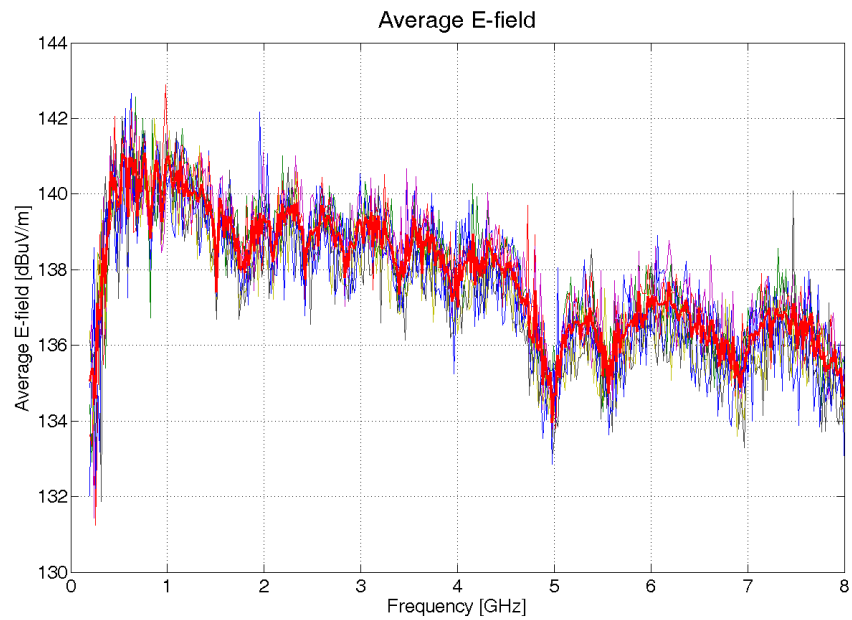


Figure 5: The average E-field measured at the eight positions in the working volume.

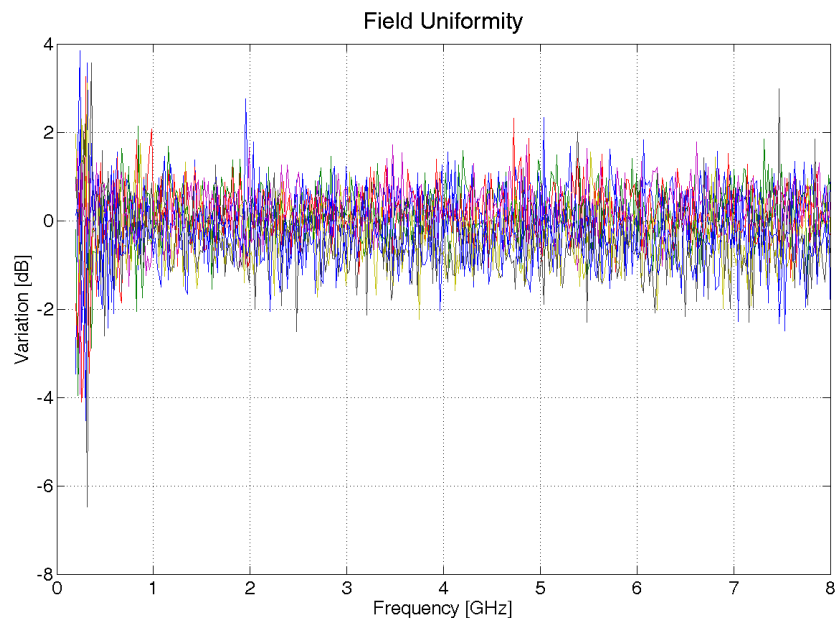


Figure 6: Normalised E-field to evaluate the field uniformity during chamber calibration.

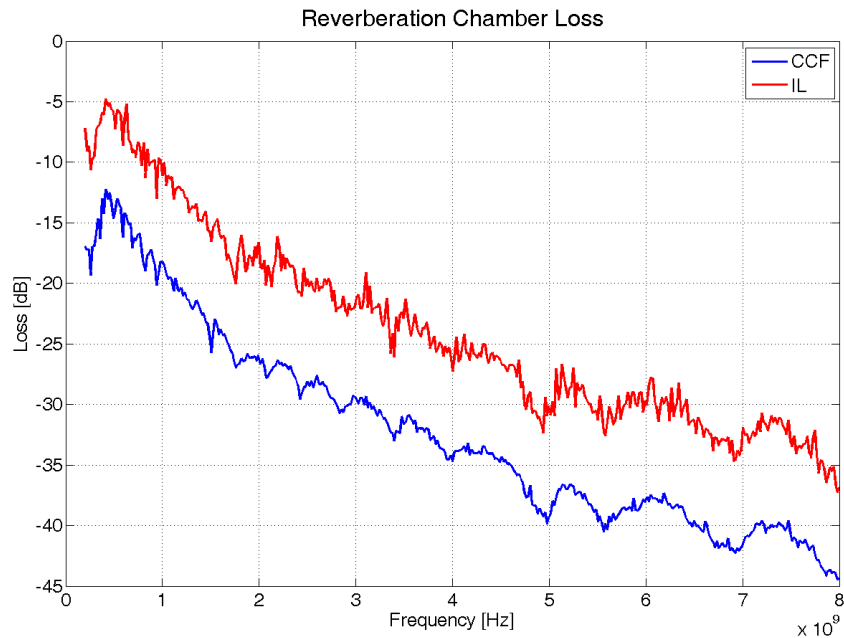


Figure 7: The attenuations of the SKA-SA reverberation chamber: *RED* is the insertion loss (IL) and *BLUE* is the chamber calibration factor (CCF).

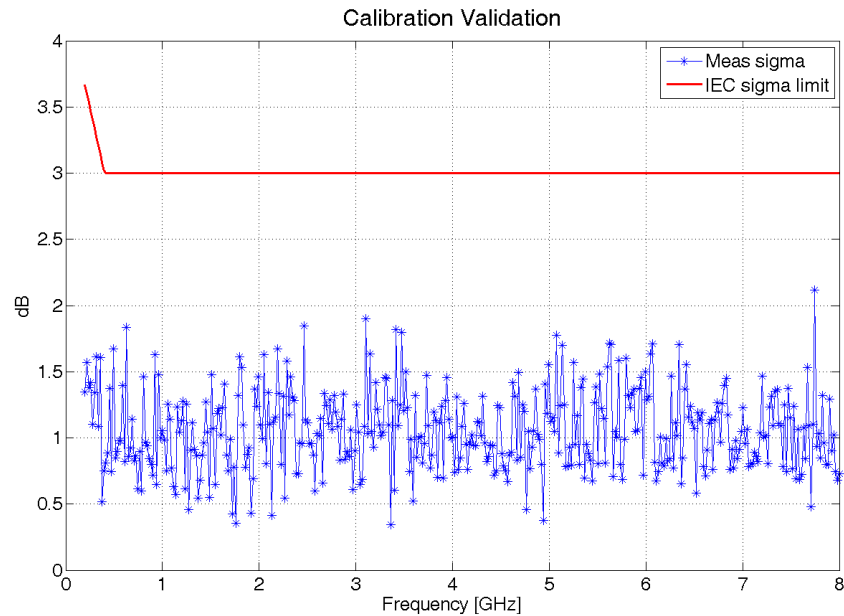


Figure 8: Measured chamber validation compared to the IEC validation requirement limits.



## 4.1 Initial Tests: ERS and Coaxial Air-Line

The emissions reference source (ERS) used in this investigation, shown in Fig. 9 (a) and (b), was manufactured by *Laplace Instruments*, and calibrated by the National Physics Laboratory (NPL) [3] applying the following half-space OATS configurations:

- Measurement location from ERS: 3 m
- Antenna scan height: 1 m to 4 m
- Frequency range: 30 MHz to 1 GHz
- Frequency step size: 2 MHz
- Polarisation: Horizontal and Vertical

The results the OATS E-field estimate from average and maximum field readings, compared to the ERS calibration data, are given in Fig. 11. For further validation of the chamber, the transfer impedance ( $Z_T$ ) for a coaxial airline, which is a brass cylindrical tube with a single circular hole in the shield (Fig. 10), was also measured. The  $Z_T$  results for the coaxial airline measured in the RCs of Pinelands and Stellenbosch, compared to the *Vance* theoretical model, are given in Fig. 12.

## 5 RC Metrology

### 5.1 Vector Network Analyzer

One of the most fundamental concepts in high-frequency (HF) network analysis involves incident, transmitted and reflected waves travelling along a transmission line. Network analysis is concerned with the accurate measurement of the ratios of the reflected signal to the incident signal, and the transmitted signal to the incident signal [4]. Complete characterization of devices and networks involves measurement of magnitude, as well as phase.

At low frequencies, where the wavelength of the signals are much larger than the length of the circuit conductors, a simple wire acting as a transmission line is very useful for carrying power. Current travels down the wire easily, and voltage and current are the same no matter where we measure along the wire. At high frequencies, however, the wavelength of signals of interest are comparable to (or much smaller than) the length of conductors. In this case, power transmission can best be thought of in terms of traveling waves. When the transmission line is terminated in its characteristic impedance ( $Z_0$ ), maximum power is transferred to the load. If this is not the case, a portion of the signal that is not absorbed by the load will be reflected back to the source. This results in standing waves and the envelope voltage will have different values at different positions along the line.

### VNA Calibration & Error Correction

When doing network analyzer measurements, three types of measurement errors exist that need to be corrected for:

1. Systematic Errors
2. Random Errors
3. Drift Errors

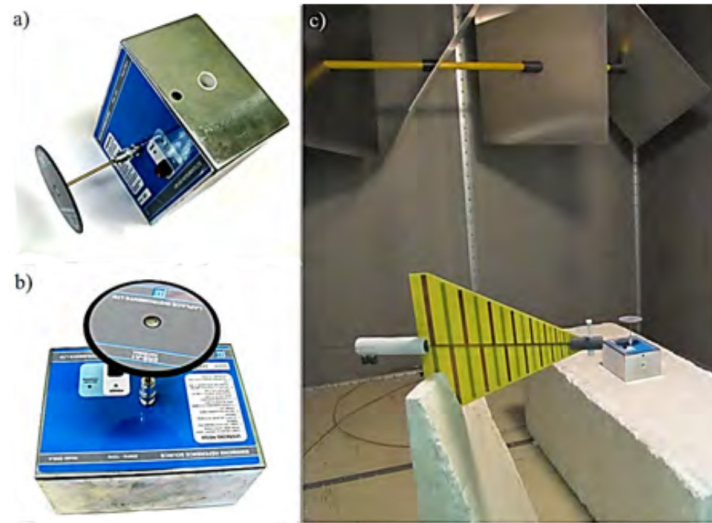


Figure 9: Estimation of OATS E-field equivalent for *Laplace Instruments LTD* emissions reference source. (a) Horizontally polarised radiator. (b) Vertically polarised radiator. (c) Equivalent OATS measurement using the KLPDA in the RC at Stellenbosch University [1].

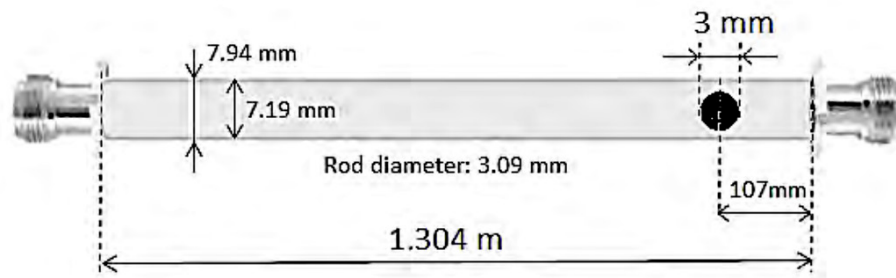


Figure 10: Geometry of the coaxial airline [1].

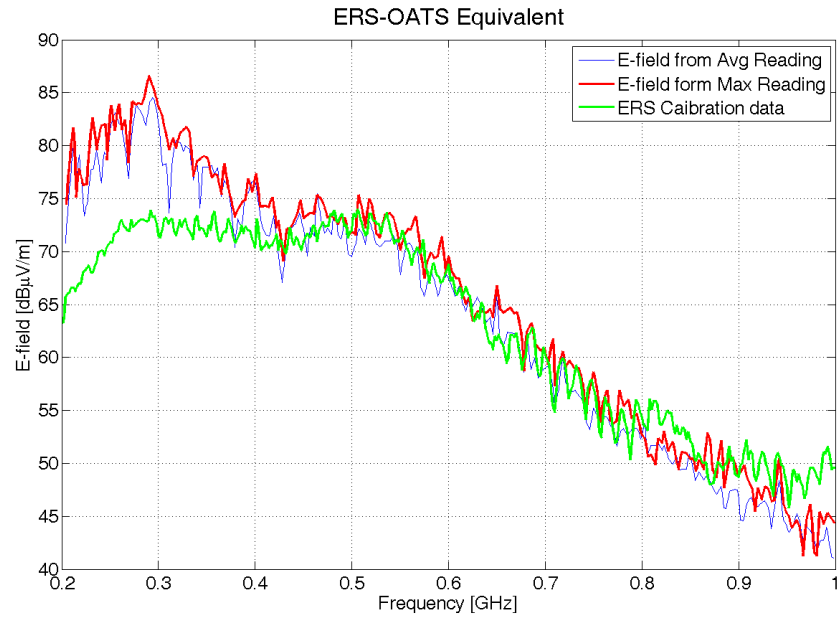


Figure 11: OATS E-field estimate from average (*BLUE*) and maximum (*RED*) readings compared to the ERS calibration data (*GREEN*).

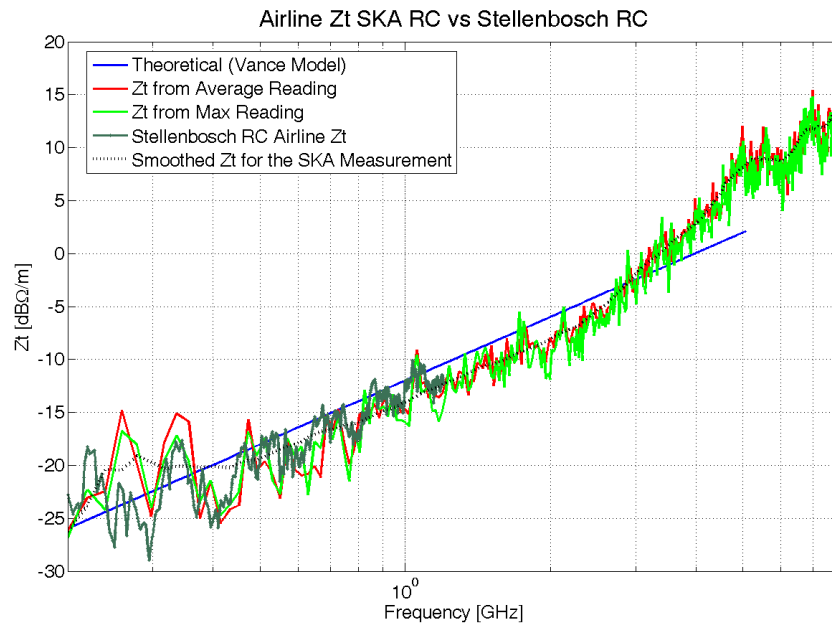


Figure 12:  $Z_t$  of coaxial airline measured in Pinelands and Stellenbosch RCs compared to the theoretical *Vance* model.

Systematic errors are caused by imperfections in the test equipment and test setup. If these errors do not vary over time, they can be characterized through calibration and mathematically removed during the measurement process. These errors are related to signal leakage, signal reflections, and frequency response. There are six types of systematic errors:

- *Directivity* and *crosstalk* errors relating to signal leakage
- *Source* and *load impedance mismatches* relating to reflections
- *Frequency response* errors caused by reflection and transmission tracking within the test receivers

The full two-port error model includes all six of these terms for the forward direction and the same six (with different data) in the reverse direction, for a total of twelve error terms. This is why two-port calibration is often referred to as twelve-term error correction [5].

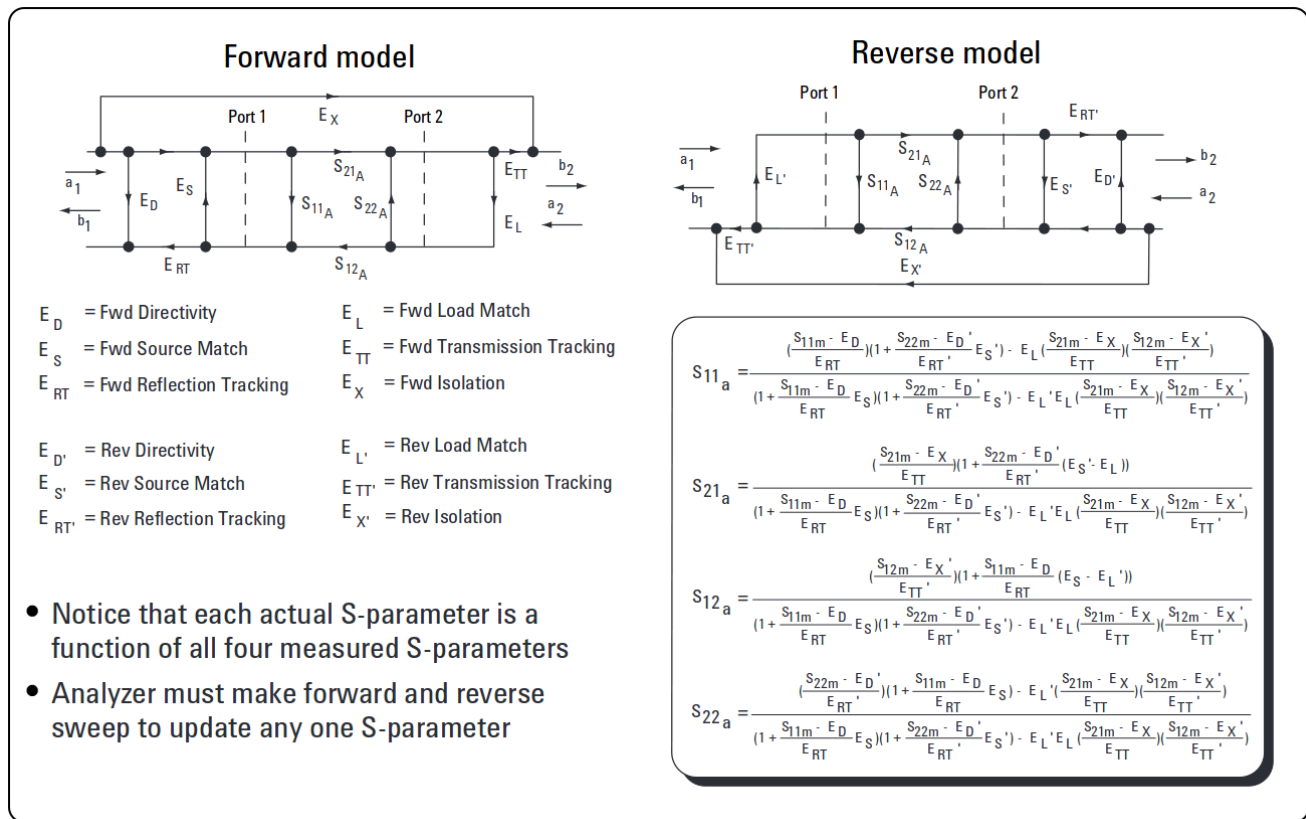


Figure 13: Two-port error correction of the 12-term error model [5].

The basis of network analyzer error correction is the measurement of known electrical standards [5]. These electrical standards include:

- Short Standard
- Open Standard
- Load Impedance Standard
- Through Standard

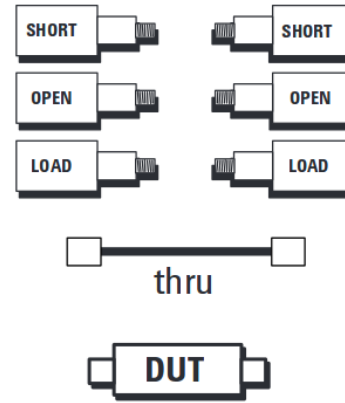


Figure 14: Full 2-port calibration standards [5].

The 2-port calibration procedure used during the RC calibration is known as the Short-Open-Load-Through (SOLT) calibration (Fig. 14). After calibration of the relevant antennas and cables, as well as the chamber insertion loss and chamber calibration factor, a DUT can be measured using a spectrum analyzer (SA) in the frequency domain (FD), or real time transient analyzer in the time domain (TD).

## 5.2 Pre-Measurement Procedure

The VNA instrument is switched on an hour before the investigation to have thermal stability and to reduce the drift of measured results with time. All connectors are cleaned with alcohol and dried with compressed air to eliminate the metallic dust left by previous usage. Furthermore, each connector is tightened with a calibrated torque wrench and the connection is re-checked every time a change was made inside the chamber [1].

## 5.3 Measurement Correction

A RC application generally involves cables and connectors for signal transport to the transmitting and the receiving antennas. Losses and mismatches are naturally inserted into the setup due to imperfections of these devices. For an effective interpretation of the results, we should correct the transmitted and the received power,  $P_{\text{input}}$  and  $P_{\text{measured}}$ , according to the following equations:

$$P_{\text{Rx}} = P_{\text{input}} \cdot L_{\text{cable Rx}} \cdot (1 - |S_{11 \text{ Ant Rx}}|^2) \cdot \text{Ant}_{\text{Rx eff}} \quad (14)$$

$$P_{\text{Tx}} = \frac{P_{\text{measured}}}{L_{\text{cable Tx}} \cdot (1 - |S_{11 \text{ Ant Tx}}|^2) \cdot \text{Ant}_{\text{Tx eff}}} \quad (15)$$

where  $P_{\text{Rx}}$  is the power received by the receiving antenna,  $P_{\text{Tx}}$  is the power radiated inside the chamber by the transmitting antenna,  $\text{Ant}_{\text{Rx eff}}$  and  $\text{Ant}_{\text{Tx eff}}$  are the receive and transmit antenna efficiencies, and  $L_{\text{cable Rx}}$  and  $L_{\text{cable Tx}}$  are the cable losses.

## 6 Conclusions

The RC of the SKA-SA was calibrated to the IEC 61400-4-21 [2] which is the relevant standard for reverberation chambers. The calibrated chamber yielded a normalised mean E-field variation within  $\pm 1.8$  dB from 200 MHz to 8 GHz, and was well below the IEC sigma limit for chamber validation. The LUF was calculated to be approximately 181 MHz.

The OATS E-field estimation of an ERS was used to validate the chamber calibration. Good correlation between the OATS E-field measured and predicted data of a well-known reference radiator (ERS) was achieved above 400 MHz. Further investigation into the sub 400 MHz over-prediction of the ERS-OATS equivalent in the Pinelands SKA-SA RC is currently underway, and will be included in the revision 1 of this document.

For further validation of the chamber, the  $Z_T$  for a coaxial airline was also measured. Good correlation between results for the coaxial airline measured in the RCs of Pinelands and Stellenbosch, compared to the *Vance* theoretical model, was achieved.

### MESA Solutions

Drs A. J. Otto and P. S. van der Merwe  
October 2013

## References

- [1] J. A. Andriambeloson, *Wideband Coaxial Transfer Impedance for Karoo Array Telescope*, Masters Thesis, University of Stellenbosch, Western Cape, South Africa, December 2011.
- [2] IEC 61000-4-21, *Electromagnetic Compatibility (EMC) Part 4-21: Testing and Measurement Techniques - Reverberation Chamber Test Methods*, October 2009, Draft.
- [3] National Physics Laboratory, *Certificate of Calibration: Laplace ERS*, Laplace Instruments LTD, October 2007.
- [4] Agilent Technologies, *Agilent Network Analyzer Basics*, Technical Document, <http://www.agilent.com/>, Last visited October 2013.
- [5] Agilent Technologies, *Agilent AN 1287-3: Applying Error Correction to Network Analyzer Measurements*, Application Note, AN 1287-3, <http://www.agilent.com/>, Last visited October 2013.